Freeze-thaw durability of novel high early strength engineered cementitious composites

by

Elliot D. Schrag

B.S., Kansas State University, 2018

A THESIS

submitted in partial fulfillment of the requirements for the degree

MASTER OF SCIENCE

Department of Civil Engineering
Carl R. Ice College of Engineering

KANSAS STATE UNIVERSITY
Manhattan, Kansas

2020

Approved by:

Major Professor
Dr. Christopher Jones

Copyright

Abstract

Concrete is susceptible to degradation due to freeze-thaw exposure, chemical attack, corrosion of embedded metals, thermal expansion, and drying and plastic shrinkage. By developing better high-performance concretes distresses from chemical, mechanical, and thermal loading can be further mitigated. High-performance concretes are characterized by their high strength and resistance to deterioration. This study investigates the durability of high-early-strength engineered cementitious composites (HES-ECC) which are known for their tensile ductility and high fracture toughness. The early strength gain was measured by conducting ASTM C39/C39M compressive strength tests and ASTM C496/C496M split tensile strength test at 4, 6, and 24 hrs. The testing showed promising results with compressive strengths above 3400 psi at six hours, and splitting tensile strengths of above 400 psi at six hours. Durability testing was also conducted by measuring the drying shrinkage according to ASTM C157/157M, freezing-and-thawing cycles according to ASTM C666/C666M, autogenous shrinkage, and adiabatic temperature rise. Measurements for the drying shrinkage test were taken at 3, 14, 28 days, 8, 10, 16, 32 weeks and resulted in high drying shrinkage due to the high cement content and absence of coarse aggregate in the mixtures. It is notable that for the mixture using Type III cement, specimens seem to expand between the 28 day test and eight and ten week tests. The mechanisms causing the expansion of the concrete are unclear but could be beneficial by reducing shrinkage cracking of concrete repairs. HES-ECC demonstrated little deterioration even after 300 freezing-and-thawing cycles. The autogenous shrinkage testing was conducted up to nine days, measuring the length change at various intervals throughout the duration of the test. Autogenous shrinkage up to approximately 0.14% length change was observed. HES-ECC reached temperatures above 176 ^{o}F for over ten hours which is concerning due to the potential of delayed ettringite formation. HES-ECC appear to be a promising repair material due to their resistance to freeze-thaw damage and high early strength development.

Table of Contents

List of Figures

List of Tables

Acknowledgments

I would like to thank Dr. Christopher Jones for his support and guidance throughout this study.

I am thankful for my committee members Dr. Christopher A. Jones, Dr. Robert J. Peterman Dr. Stacey Kulesza for taking the time to go through my thesis.

Finally, I would like to thank Faisal, Poornima, Ragini, Subdoth, Ben and Cody for their help in conducting the experimental work of this research.

Dedication

First, to my parents Lowell and Betty Schrag. I could never have done this without your love, encouragement, and constant support. Thank you for teaching me to work hard, love others, and to love God. I also dedicate this thesis to my sisters Elisa, Abbie, and Ariel, as well as to my brothers Aaron, Kendall, and Thomas. To my best friends, Chris and Naomi, who brought tremendous joy to the journey. Soli Deo Gloria.

Chapter 1 - Introduction

1.1 Overview

Concrete structures are subjected to various types of loading that results in deterioration, damage, and defects, in both new and repaired concrete structures (Li and Li, 2011). Environmental and mechanical loading (e.g., freezing and thawing cycles, chemical attack, restrained shrinkage, and fatigue) causes deterioration of the concrete during the service life. Short-term severe loading damages the concrete and results in cracking, spalling, bond splitting, or complete failure of the concrete structure or element (Li and Li, 2011). These loading conditions include earthquakes, impacts, fires and overloading. Defects in the concrete structure are a result of poor construction practices, improper detailing or design, human error, poor quality control of materials that lead to insufficient structural capacity and premature deterioration (Li and Li, 2011). In order to extend the service life of concrete structures that have lost durability due to deterioration, damage, and defects, efficient and effective repairs are required (Emmons, 2006).

Premature failure of concrete repairs can lead to significant life-cycle economic, social, and environmental impacts due to frequent maintenance and repairs throughout the service life of the concrete structure (Li and Li, 2011). In the U.S. alone, it is estimated that concrete repairs (including strengthening and protection) cost owners $18 to $21 billion annually (Emmons, 2006). The 2017 infrastructure report card by the American Society of Civil Engineers states that there is a $2 trillion investment gap in infrastructure that will be needed by 2025 (ASCE, 2017). The report card goes on to state that due to underfunding there is a backlog of $836 billion needed for highway and bridge capital (ASCE, 2017). Repair of existing highways make ups $420 billion of this backlog and another $123 billion for bridge repair (ASCE, 2017). Furthermore, U.S. motorist spent $533 per a driver on additional repairs and operating costs in 2015 and, in 2014, due to traffic congestion and delays an estimated $160 billion was lost due to wasted time and fuel (ASCE, 2017). Based on recent studies, the dominant influencers of life-cycle social costs and

environmental impacts on concrete infrastructure are traffic congestion and repair operations. The next largest contributor is material production which is influenced by repair operations and repeated maintenance (Keoleian et al., 2005).

The use of high early strength (HES) concrete materials has become common for concrete pavement repairs because they reduce the amount of lane closure time and thus traffic disruption is minimized (Wang and Li, 2011). For example, it is often required by transportation authorities that a lane be reopened for morning traffic which means a job must be completed in six to eight hours at night (Wang and Li, 2011). Extensive research has been conducted in the past few decades on HES concrete materials which has led to the development of a variety of concrete mixtures which meet minimum requirements for concrete pavement repair. These concrete mixtures are able to achieve high-early-strength by incorporating proprietary rapid setting cements or accelerating agents with Type III portland cement into the concrete mixture. However, concrete materials are prone to crack which leads to a reduction in the durability properties of the concrete. Repair sites that use HES concrete are known to fail prematurely and most failures are attributed to a lack of durability (Wang and Li, 2011). The mechanisms of deterioration that cause a reduction in the durability properties are environmental (e.g., shrinkage, freezing-thawing cycles, chemical intrusion, and corrosion), external (e.g., poor construction practices and workmanship), and mechanical (e.g., fatigue) effects (Li and Li, 2011; Sahmaran et al., 2013).

A special class of high-performance fiber-reinforced cementitious composites are engineered cementitious composites (ECC) which are highly ductile (Sahmaran et al., 2013). The high ductility of ECC is achieved through the development of multiple tight-width cracks (less than a 100 microns) that enable strain hardening behavior in the material (Li et al., 2001). ECC can be tailored (or engineered) based upon micromechanical models that relate macroscopic properties to the microstructure of a composite, in order to get the desired performance of the material (Li, 2004). ECC are expected to be an effective repair materials due to (1) their ability to maintain tight crack widths upon loading which would minimize the intrusion of unwanted substances, (2) high ductility/deformation compatibility with concrete substrate structure, and (3) high-fracture toughness which allows it to defuse and arrest unstable crack propagation (Wang and Li, 2006).

This study investigated the durability of high early strength engineered cementitious composites (HES-ECC). The primary objective was to determine if HES-ECC are a high performing and durable material. The experimental investigation involved the durability testing of four different mixture which allowed for comparison and future optimization of mixtures.

1.2 Background

HES concretes are used for concrete repair since they minimize operation disruption by allowing a facility to quickly reopen after a repair. Concrete structures such as bridge decks, parking structures, highway pavements, and airport runways are often repaired with HES concretes to minimize operation disruption (Li and Li, 2011). The premature failure of repaired concrete structures is a global concern because it leads to costly and time-consuming repairs. The US Army Corps of Engineers, based on an inventory of concrete structures, estimated that a little more than 50% of the concrete repairs perform satisfactorily (Taffese and Sistonen, 2013). By developing new materials that are sustainable, high performing, and durable, the economic, environmental, and social burdens will be alleviated. A material such as HES-ECC may be able to serve this purpose.

1.3 Problem Statement

HES concrete materials develop strength (compressive and flexural) rapidly which gives them the desired mechanical properties for many applications. These materials, however, are more prone to early-age cracking due to higher thermal and autogenous shrinkage caused by faster hydration and heat release (Bentz and Peltz, 2008; Mehta, and Burrows, 2001; Mihashi, et al., 2002). These materials are also less resistant to freezing-and-thawing which limits their application in colder regions (Li and Li, 2011; Qadri and Jones, 2020; Porras et al., 2020). Another important mechanism of deterioration is caused by delayed ettringite formation (DEF) which occurs when

high early temperatures reach above 158-176 °F due to early-age heat release during hydration (Lim et al., 2016). Due to the high cement content and accelerating admixture usage of HES concrete and the associated heat evolution of the hydrating cement, DEF may be an important deterioration mechanism. Durability problems also occur in concrete repairs due to the restraint of the concrete repair by the concrete substrate which causes debonding and cracking of the concrete repair (Li and Li, 2011). This experimental investigation attempts to address these issues by conducting durability testing on HES-ECC.

1.4 Objective

The primary objective of this study was to test the durability of high-early strength engineered cementitious composites and to verify that HES-ECC is a high-performance material. This was done in two phases. Phase one compiled existing research on the background of the durability of HES-ECC. Phase two was testing the various mixtures to ensure adequate early strength gain. Also, the durability was tested by measuring the drying shrinkage, autogenous shrinkage, semi-adiabatic temperature rise, and damage from freeze-thaw cycles.

1.5 Research Methodology

The mixtures chosen for this research were based off research previously conducted on HES-ECC. Strength testing was then conducted to verify that the chosen mixtures would develop high-early strengths. The strength tests included compressive (ASTM C39) and split tensile (ASTM C496). The compressive and split tensile strengths were tested at 4 hours, 6 hours, and 24 hours.

Durability tests included length change (ASTM C157/C157M), freeze-thaw resistance (ASTM C666), autogenous shrinkage, and semi-adiabatic temperature rise. The autogenous shrinkage was measured by casting 3 in. × 4 in. × 16 in. prisms and attaching linear variable differential transformers (LVDTs) to each end and taking measurements every 5 minutes for 4 hours, then every 30 minutes for 24 hours, and then every hour for 7 days. The semi-adiabatic temperature rise was measured by placing a HES-ECC cylinder into an insulated container

immediately following batching. The temperature of the HES-ECC was measured for two days until the internal temperature was similar to room temperature.

1.5.1 Mixture Design

This study tested four different HES-ECC mixtures. In order to ensure consistency of the mixtures and only vary the type of cement, each mixture contained the following:

- Water-to-cementitious material (w/cm) ratio of 0.34 (except for one mixture which had a w/c ratio of 0.4)
- FA-A sand
- ADVA® 140M type A/F water reducer or EUCLID® Plastol 6400 type A/F water reducer
- Calcium chloride (accelerating admixture)

The four mixtures had one of the following types of cement or cement blends:

- Type III portland cement
- Type III Portland cement with 8% Metakaolin
- Type III portland cement with 15% Metakaolin
- CSA/Type III portland Cement Blend

1.6 Thesis Outline

This thesis includes seven chapters. Chapter 1 includes an introduction to the research. Chapter 2 consists of a literature review, history and development of engineered cementitious composites. The literature review also examines the durability of ECC and durability test methods. Chapter 3 discusses the materials used for all designed concrete mixtures. Chapter 4 consists of the mixture proportioning and laboratory testing. Chapter 5 details the results of the research, Chapter 6 includes analysis and discussion. Chapter 7 covers the conclusions.

Chapter 2 - Literature Review

2.1 History and Development of Engineered Cementitious Composites (ECC)

Since 1990, researchers and practitioners have been contributing to the development of the design theory, material processing, material mechanical and durability characteristics, structural design basis, structural element performance, and full-scale infrastructure design and construction of Engineered Cementitious Composites (ECC). The body of knowledge on ECC continues to increase as the material undergoes advances that add value and further improvements.

2.1.1. What is ECC?

ECC is a special type of fiber reinforced concrete (FRC) that is characterized by being ductile, with tensile strain capacity beyond 2% (Li 1993). This is achieved by a unique design method that uses ECC micromechanics to systematically tune the material microstructure for synergistic interactions between the microstructural components. In other words, by tailoring or *engineering* the fiber, the matrix, and fiber/matrix interface to interact in a prescribed manner upon loading high ductility is achieved (Li, 2003). This is also the reason for the name *Engineered* Cementitious Composites.

2.1.2 Design Basis for ECC

ECC have a unique design basis that is distinct from high strength concretes which achieves high compressive strengths by tight particle packing. The design basis for ECC is a micromechanical model that relates the microstructure to the macrostructure by synergizing the mechanical interactions between fiber, matrix, and interfaces of the composites. By engineering these composites, it is possible to obtain high ductility as a result of the strain-hardening behavior of ECC after first cracking. Upon cracking, the material will distribute the force back into the matrix resulting in multiple cracks making the tensile deformation nonlocalized. In contrast, fiber

reinforced concrete (FRC) exhibit tension-softening behavior where tensile deformation is localized to the site of the first crack. The formation of multiple microcracks, which typically have crack widths less than 100 μm, in ECC gives it tensile ductility and resistance to chemical intrusion (Li, V.C., 2019).

Li, V.C. (2003) reported on the micromechanics-based design concept for ECC: fiber reinforced cementitious composites have a fundamental property that relates the average tensile stress transmitted across a crack, σ, with a uniform crack opening, δ, called the fiber bridging property across cracks (Li, 2003). This fundamental property links the material constituents and the composites tensile ductility. The role of load bearing and energy absorption in fiber bridging is crucial to understanding the strain-hardening behavior of ECC. These are the basis for the two criteria that govern the development of multiple-cracking in ECC: 1) the strength criterion - the maximum bridging stress must be greater than the matrix cracking strength and 2) the energy criterion.

The energy criterion is not as straightforward as the strength criterion and will be explained in more detail. Figure 2-1 illustrates the σ - δ curve and the concept of complementary energy.

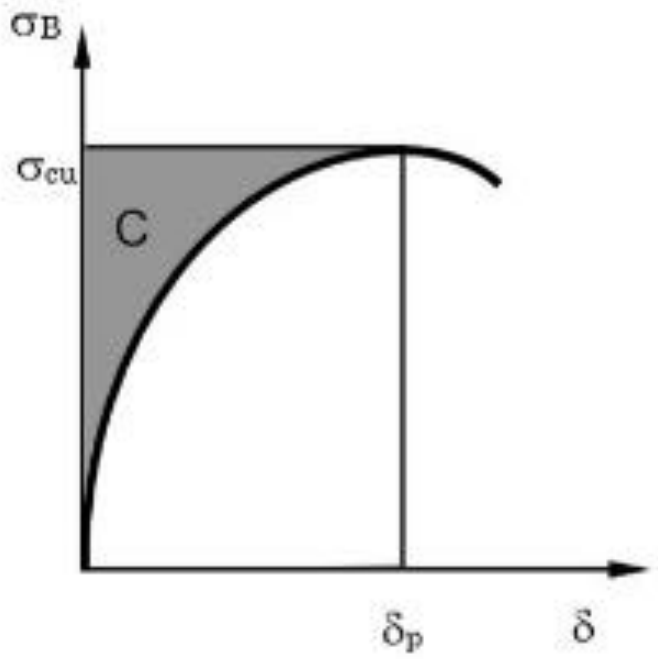

Figure 2-1: The average tensile stress vs uniform crack opening, σ - δ curve, and the concept of complementary energy (Li, V.C., 2003).

The fiber/matrix interface must not be too weak or too strong, if the fiber/matrix interface is too weak the fibers will pull-out resulting in a low peak strength, σ_{cu}. In contrast, if the fiber/matrix is too strong the fiber will rupture and have a small critical crack opening, δ_p. In both cases, the complementary energy will be low as seen in Figure 2-1. A high complementary energy allows the crack to remain flat as it propagates and maintain tensile load capacity after cracking. Another crack can develop from a load transferring through the crack plane back into the matrix and will result in multiple cracking if the process is repeated. Since the shape of the σ - δ curve is critical for developing a high complementary energy, it is important to control the fiber and fiber/matrix interaction parameters which govern the shape of the σ - δ curve. The fiber parameters include the fiber diameter, length, strength, modulus, and volume fraction. The chemical and frictional bond properties are the fiber/matrix interaction properties of interest. By controlling these parameters, the microstructure of ECC can be engineered to have the desired quality of high ductility and multiple crack behavior.

2.1.3 High Early Strength Engineered Cementitious Composites (HES-ECC)

ECC mixtures conventionally use Type I ordinary portland cement (OPC), however, when high early strength development is needed other binder systems must be considered. The use of proprietary rapid hardening cements, Type III OPC, and accelerating admixtures have been used to develop high early strength. It also common in high early strength concrete to have a high cement content and low w/c ratio since these both influence the strength of the concrete (Shanahan et al., 2016). HES-ECC utilizes these rapid hardening cements and admixtures to develop high early strength while maintaining tensile ductility through tuning of the mixture based off the micromechanical model.

Research conducted by Wang and Li (2006) investigated HES-ECC with an emphasis on the material design aspect. Their research explored the use of rapid hardening cements and normal portland cement in HES-ECC. They concluded that the matrix fracture toughness evolves at a faster rate than the interface frictional stress, chemical bond and slip-hardening coefficient of polyvinyl alcohol (PVA) fiber leading to a reduction in the strain hardening behavior, and thus a loss in ductility. The loss in ductility was overcome by the incorporation of polystyrene beads into the mixture which created artificial flaws that resulted in nearly saturated multiple-cracking. The mixtures that used Type III portland cement and calcium sulfo-aluminate were able to develop compressive strengths of more than 3000 psi in three hours and retain tensile strain capacity of more than 2.0% which is desired when high early strengths are needed.

In subsequent research by Li and Li (2011), the mechanical and shrinkage properties of HES-ECC based on Type III portland cement were evaluated. Their study concluded that HES-ECC possessed high early age compressive, flexural, and tensile strength as well as large tensile ductility with controlled microcrack width. The experimental investigation measured the drying shrinkage according to ASTM C157/C157-99 and ASTM C596-01 and also by using the restrain shrinkage ring test following AASHTO PP-34-99. Based off these experiments, HES-ECC had a

drying shrinkage of approximately twice that of ordinary HES-Concrete due to the high cement content, fineness of cement particles, and absence of coarse aggregate. However, the shrinkage strain was 0.3% which was much lower than the tensile strain capacity of 3 to 6% of the HES-ECC. The restrained shrinkage ring test revealed that when HES-ECC are restrained the material's ductility can accommodate for the shrinkage deformation by forming multiple microcracks without localized fracture failure.

2.2 Durability of ECC

Traditionally, structural engineers relied on concrete to primarily carry compressive loads, however, in field conditions concrete is subjected to tensile stresses from mechanical and environmental loading such as shrinkage, thermal effects, and chemical attacks (Sahmaran, 2009). These tensile stresses lead to cracking of the concrete which causes durability problems by reducing load-carry capacity and allowing the intrusion of water and other unwanted substances into the concrete. The loss in durability of concrete results in the deterioration of concrete structures and infrastructure, leading to costly repairs and maintenance. The improvement of the durability of concrete has been addressed by modifying the concrete using air entrainment, sulfate resistant cements, or minimum reinforcement, but none of these addresses the inherent brittleness of concrete (Lepech and Li, 2006). The development of high-performance fiber-reinforced cement-based composites (HPFRCC) has been shown to greatly enhance the durability and long-term performance of concrete structures (Lepech and Li, 2006). ECC falls in this class of material and due to the formation of multiple tight-widths crack under loading behaves like a ductile material.

A high-performance concrete will be able to resist mechanical, chemical, thermal, and combined loading. Extensive research has been conducted on the durability of ECC and their ability to resist these types of loading. Since ECC may be used with steel reinforcement the protection of the steel reinforcement against corrosion will be considered in the durability of the system. This section aims to summarize this research by discussing the (1) durability of ECC under mechanical loading, (2) the durability of ECC under chemical loading, and (3) the durability of ECC under thermal loading.

2.2.1 Durability of ECC under Mechanical Loading

An important property of the structural durability of concrete is the control of crack widths under loading. The cracking of concrete leads to the ingress of unwanted substances. This is a major concern for reinforced cementitious composites because corrosion of the reinforcement can lead to costly repairs and replacement of reinforced concrete. Since ECC form multiple tight-width cracks upon loading, they should have better durability than ordinary concrete. Also, the ductility of ECC is a function of the formation of multiple tight-width cracks and not plastic deformation as is the case for steel (Ziji et al., 2012).

Li et al. (2001) showed that ECC have a maximum crack width under 100 μm with a tensile strain greater than 4.0%. Other studies by Weimann and Li (2003) and Wang and Li (2006) gave similar results of tight crack widths and high tensile strains. All these studies used PVA fibers at 2.0% to 2.5% the total volume. In the study by Li et al. (2001), the increase in volume fraction from 2.0% to 2.5% showed a minor reduction in crack width. This study also indicates that an increase in the amount of aggregate reduces the tensile ductility and that a reduction in the chemical and frictional fiber bond gives a higher tensile strain capacity. The replacement of cement with fly ash gave similar crack widths to mixtures without fly ash (Wang and Li 2006).

Structures subjected to cyclic loading or high sustained loads need to maintain tight crack widths to meet service conditions (Ziji et al., 2012). If cracks are not restricted, they will go beyond the threshold width causing a large increase in moisture, gas, and chloride ingress (Ziji et al., 2012). In a study by Jun and Mechtcherine (2007), specimens were tested under monotonic and cyclic tensile loading and creep tests were also performed. The results of the experiment indicated little difference in the number of cracks under the different types of loading. The largest deviation was when the specimen was loaded under deformation controlled cyclic loading showing approximately 20% lower average number of cracks. In another study by Boshoff (2007), Pre-cracked ECC specimens were subjected to tensile creep tests. The specimens were first subjected to a tensile deformation causing an average strain of 1% which simulates a large live load. This

was followed by tensile creep loads of 30%, 50%, 70%, and 80% of the ultimate tensile strength. The results of the experiment showed that fewer cracks formed under creep loading compared to monotonic deformation-controlled tensile loading at the same amount of deformation. For sustained loads at 80% the ultimate tensile strength, wider cracks with larger crack widths were measured. Boshoff et al. (2009) in a different study, concluded from performing single fiber pull-out tests under monotonically increasing pull-out displacement and under tensile creep load that time-dependent fiber slip is a mechanism of tensile creep deformation and time-dependent crack width increase. Yu et al. (2018) investigated the rate-dependent tensile properties of ECC. In this experiment, specimens were loaded in direct tension at loading strain rates between 0.00001 to 0.05 s-1. The rate of loading has nominal impact on the crack widths of specimens. A higher ratio of fiber length to fiber diameter increased the number of cracks but decreased the crack width and crack spacing.

The prevention of degradation of the matrix and corrosion of the reinforcing bars is done by minimizing the ingress of moisture, gas, and salts (Ziji et al. 2012). Moisture ingress and migration is controlled by moisture diffusion and capillary sorption (Neithalath 2006, Bazant et al. 1971). Capillary absorption is greatly reduced in UHPFRC by densification of the matrix and in ECC the diffusivity is reduced by inherent crack control (Kunieda et al. 2007, Lepech and Li 2005, Sahmaran et al., 2005). Several studies have shown that the permeability was reduced in fiber reinforced cementitious composites compared to plain concrete (Rapoport et al. 2001, Maalej et al. 2002, Miyazato and Hiraishi, 2005). These studies indicated that crack widths under 100 μm had negligible difference in permeability. Chloride penetration and permeability of ECC in comparison to mortar were investigated by Sahmaran et al. (2005). The study showed that since ECC maintained tight crack widths after flexural deformation and that they had a much lower chloride diffusion compared to the mortar. These studies conclude that ECC are effective at slowing down diffusion of chloride ion under mechanical and environmental loading, by its ability to develop multiple tight crack widths.

2.2.2 Durability of ECC under Chemical Loading

ECC ability to maintain narrow crack widths under applied loading may provide good resistance to penetration of deleterious materials even after straining. This section will discuss the impact of chemicals on ECC. Exposure of reinforced concrete members to chloride environments can lead to corrosion of the steel reinforcement and eventually spalling of the concrete. Corrosion of the reinforcement progresses by depassivation of the protecting layer; the expansion of the corrosive products from the oxidized steel cracks the concrete cover which leads to increased exposure, and thus faster corrosion (Ziji et al., 2012). Sahmaran et al. (2008) investigated the corrosion of R/mortar and R/ECC by performing an accelerated corrosion test by an electrochemical method. Residual flexural load tests were performed on the specimens after exposure to a chloride environment and the mass loss of the steel rebar was measured. The results of the experiment concluded that ECC had a high resistance to spalling compared to conventional mortar and after 50 hours of accelerated corrosion exposure was able to retain nearly 100% of its flexural capacity. ECC higher resistance to corrosion can be attributed to its high tensile strain capacity, strain hardening, and multiple-cracking behavior. Kabele et al. (2006, 2007) performed single fiber pull-out and nano-indentation tests on specimens exposed to chloride environments. The results of the single fiber pull-out test showed a reduction in chemical bond of the fibers and a slight increase in frictional bond after being subjected to chloride attack. The matrix fracture toughness was almost unaffected by chloride attack, but there was reduction in the modulus of rupture. This is most likely due to the decrease in the fiber-bridging effectiveness.

Soft water or water containing sulfur or ammonium ions can cause calcium leaching which decalcifies the matrix and degrades the mechanical properties of the cementitious composite (Ziji et al., 2012). Němeček et al. (2006) investigated the degradation processes of ECC by exposing ECC specimens to 1.4 mol/L of KNO_3 for 16 days. After the specimens were exposed to the accelerated leaching process, nano-indentation measurements were taken and showed a reduction in the modulus of elasticity compared to the control specimens. Another study by Němeček et al.

(2007) confirmed these results by using nano-indentation on specimens exposed to NH_4NO_3 for 70 days. ECC specimens exposed to NH_4NO_3 at room temperature were tested using the single fiber pull-out test by Kabele et al. (2006). The tests resulted in significantly reduced pull-out strengths compared to the control specimen. These tests indicate that calcium leaching severely damages the ECC matrix.

Li et al. (2004) study the impact of hot and humid environments on ECC. Specimens were made with multiple fibers and with a single fiber. The specimens were immersed in water at 60 ^oC for 0, 4, 13, and 26 weeks. After exposure to the hot water fiber pull-out test and uniaxial tensile tests were performed on the specimens. The results of the experiment showed that the hot water immersion test had minimal impact on the fiber parameters: fiber strength, fiber stiffness, and fiber elongation. However, the chemical bond of the fibers and mortar increased, and the apparent fiber strength decreased. These are indicators of the long-term durability of ECC under hot and humid environments. Long-term exposure to hot water immersion lead to an increase in tensile strength, but the tensile strain was reduced from 4.5% to 2.7% after 26 weeks of hot water exposure. ECC can be designed to be durable if the long-term tensile strain values are used during structural design.

Sulfate attack is considered a critical deterioration mechanism affecting the durability of concrete structures. When concrete is exposed to sulfate solution, the cement hydration products react with sulfate ions creating an expansive product that leads to cracking of the concrete (Liu et al., 2017). In turn, the cracks lead to more sulfate penetration and thus accelerating the deterioration. Liu et al. (2017) studied the durability of ECC in sulfate and chloride environments. The study specifically investigated ECC under sulfate and combined sulfate-chloride conditions. ECC and mortar specimens were made and then exposed to a solution of 5% Na_2SO_4 and a combined solution of 5% Na_2SO_4 + 3% NaCl for 30, 60, 90, 120, 200, and 420 days. The findings of the study showed that ECC remained durable for 420 days of exposure under both environmental loading conditions. The mortars, however, showed notable deterioration under the same exposure conditions. ECC exposed to long-term sulfate and sulfate-chloride conditions exhibited an increase in tensile and compressive strength, but a reduction in tensile strain. Nonetheless, ECC still had a tensile ductility above 2% after 200 days of exposure and maintained multiple cracking and strain-hardening behavior. The observed composite behavior is a result of

an increase in the matrix fracture toughness and interfacial frictional bond, and a decrease in the fiber/matrix bond after chemical exposure. The study indicates that ECC could potential enhance the life of hydraulic structures under aggressive sulfate or sulfate-chloride environments.

Ziji et al. (2012) reported that a limited type of fibers (PVA, polyester, alkali resistant (AR) glass and E glass) were tested by immersing them in high alkaline hot water (80 ^{o}C) for 14 days. The PVA fibers were able to retain almost full strength. Fibers were also tested in solutions of diluted sulfuric acid, hydrochloric acid and nitric acid in water for more than 1 year. The largest reduction in tensile strength was 5%. Sahmaran and Li (2008) did an experimental investigation on the performance of ECC in highly alkaline environments in accordance with ASTM C1260. After 30 days of soaking no expansion of the ECC specimen was observed. This is most likely due to the non-reactive silica sand used in the ECC mixture. In the case where a reactive sand and alkalis are present in ECC, expansion caused by alkali-silica reaction is improbable if a high volume of fly ash is used.

2.2.3 Durability of ECC under Thermal Loading

Structures build with cementitious materials are susceptible to extreme temperatures such as exposure to fire or freeze-thaw cycles as well as large thermal gradients (Ziji et al., 2012). These events can cause structural durability problems if not properly addressed. Sahmaran et al. (2010) tested 50 mm cubed ECC specimens at temperatures of 200 ^{o}C, 400 ^{o}C, 600 ^{o}C, and 800 ^{o}C to determine the impact of high temperatures on the mechanical and microstructural properties of ECC. The PVA fibers used in the experiment had a melting temperature of 230 ^{o}C. All specimens were tested under compression and a mercury intrusion porosimetry technique was used to define the pore size distribution at the respective temperatures. At 200 ^{o}C the specimen had a reduced compressive strength and stiffness of approximately 15%, but the microstructure showed no prominent changes. Increasing the temperature to 400 ^{o}C the strength reduction was still around

15%. It was also observed at both 200 ^{o}C and 400 ^{o}C that the supplementary pores and small channels developed in the ECC matrix due to melting of the PVA fibers. At 400 ^{o}C hairline cracks were observed at the surface of the specimen. A reduction in compressive strength of 53% was observed after exposure to a temperature of 600 ^{o}C. Surface cracking was also more prominent at this temperature. Further strength reduction occurred after exposure to temperatures of 800 ^{o}C, with strengths approximately 34% the unheated control specimen. For temperatures above 400 ^{o}C, deterioration of hydration products and sand become prominent factors in determining the mechanical properties of ECC, not just physical change such as increase in total intruded porosity, the average pore diameter, and surface cracking. It was also observed that at temperatures above 400 ^{o}C the material stiffness rapidly declined compared to the compressive strength. The results of this experimental investigation compared to data given from research articles on normal concrete and fiber-reinforced concrete indicated that ECC performed similar or better than fire-damaged plain concrete with steel and/or polypropylene fibers.

In a subsequent study by Sahmaran et al. (2011), the effect of fly ash and PVA fiber on the microstructure and residual properties of ECC exposed to high temperatures was examined. Similar to the previous study, 50 mm cubed ECC specimens were exposed to temperatures of 200 ^{o}C, 400 ^{o}C, 600 ^{o}C, and 800 ^{o}C. However, the specimens were made with either 55% or 70% of fly ash by weight of the total cementitious material. The increase in fly ash from 55% to 70% showed better residual mechanical properties after being exposed to temperatures from 200 ^{o}C to 600 ^{o}C. At temperatures of 800 ^{o}C, however, the effect of the additional fly ash was lost. It was also reported that ECC with PVA fibers had high resistance to thermally induced explosive spalling. Furthermore, when ECC where exposed to air cooling no spalling occurred, even at temperatures of 800 ^{o}C. This study also gave similar results to the previous study on the compressive strength, Sahmaran et al. (2010).

The influence of heating duration and cooling regimes on the macromechanical properties and microstructure of ECC specimens exposed to temperatures up to 800 ^{o}C was investigated by Yu et al. (2014). The specimens were exposed to temperatures of 200 ^{o}C, 400 ^{o}C, 600 ^{o}C, and 800 ^{o}C followed by cooling by quenching in water or cooling in air. The experiment concluded that at 200 ^{o}C the compressive strength and stiffness increased with increasing heating duration. In contrast, at temperatures above 200 ^{o}C the compressive strength and stiffness decreased as the

heating duration increased. Also, the specimens quenched in water regained compressive strength and stiffness after being exposed to high temperature. This is due to the rehydration of cement particles which produce more crystals to fill the internal cracks and thus increase the strength of the matrix. The cross-section of the specimens cooled in air were much coarser because they did not experience further hydration like those quenched in water. Significant degradation of mechanical strength and stiffness as well as significant changes in microstructure and pore size distribution occurred at a temperature of 600 ^{o}C, indicating it to be a critical temperature for the durability of ECC.

Mechtcherine et al. (2012) investigated the effects of strain rate and elevated temperatures on the tensile behavior of ECC. The ECC specimens were tested at 60 ^{o}C, 100 ^{o}C, and 150 ^{o}C in order to simulate condition such as hot weather with solar radiation or operations in a power plant. The specimen tested at 60 ^{o}C showed increased strain capacity, but a decrease in tensile strength. This is a result of the reduction in fiber/matrix bond strength which causes higher elastic and plastic deformation of fibers leading to larger cracks. In comparison, at 100 ^{o}C the strength decreased and strain capacity increased with increasing strain rate. The combination of temperature and strain rate on the bond and fiber properties are favorable for the strain capacity of the composite in this case. At a temperature of 150 ^{o}C there was a considerable loss in fiber strength leading to a loss in ductility and the ability of ECC to form multiple cracks.

Freezing and thawing cycles can seriously impact the durability of concrete structures. For this reason, Sahmaran et al. (2009) investigated the durability of ECC under freezing and thawing cycles. The tests were conducted according to ASTM C666. Also, the air-void and pore size distribution were measured according to ASTM C457 and by mercury intrusion porosimetry, respectively. The ECC with fibers was able to easily survive 300 freezing and thawing cycles. After exposure to freezing and thawing cycles, the ECC only had a slight reduction in ductility and flexural strength. This is explained by the larger pore sizes and the intrinsically high tensile ductility and strength of ECC. It should also be noted that no air entrainment was purposefully

added to the ECC mixtures. In subsequent study, Sahmaran et al. (2011) conducted the same tests on ECC with a high volume of fly ash. ECC mixtures were prepared by replacement of cement with either 55% or 70% fly ash by weight of the total cementitious composites. It was concluded that incorporating fly ash in the mixture slightly reduced the mechanical performance of ECC due to the lower compressive strengths. However, they still showed good durability performance under freezing and thawing cycles. In a different study by Yon et al. (2011) the tensile behavior of ECC with PVA or PE fibers after freezing and thawing was evaluated. The specimens were tested under monotonic tension loading and cyclic tension loading after 0, 100, and 200 cycles of freezing and thawing. The results indicated that after 200 cycles of freezing and thawing the ECC specimens, the specimens were stiffer with a slight reduction in the inelastic strain. Under monotonic and cyclical loading, the ECC specimens showed an increase in tensile strength and a decrease in tensile strain capacity.

Autogenous shrinkage and thermal gradients cause cracking at early ages of concrete by inducing tensile stresses in the material. Hydration reaction of the cement is exothermic and is the origin of these phenomena in concrete. Also, the material properties (strength, modulus of elasticity, autogenous shrinkage, and creep) are dependent on the hydration reaction (Ziji et al., 2012). Sahmaran et al. (2009) investigated the prevention of autogenous shrinkage by internal curing. The substitution of silica sand with 10% and 20% saturated lightweight aggregates (LWA) (by weight of total silica sand) were used in the ECC mixtures. The specimens also had two different fly ash contents (FA/PC of 1.2 and 2.2 by weight). The autogenous shrinkage, drying shrinkage, compressive strength, flexural strength, and direct tension were all measured. It was concluded that the saturated fine LWA were able to reduce the autogenous shrinkage by 67% when compared to the control specimen at 28 days and 37% reduction of drying shrinkage at 90 days. However, the partial replacement of silica sand with LWA did adversely affect the strength and ductility properties of the ECC. Nonetheless, a strain capacity of 2% was observed which is 200 times greater than conventional concrete. The incorporation of fly ash reduced both autogenous and drying shrinkage; the specimen with higher amounts of fly ash had lower drying shrinkage and autogenous shrinkage.

The drying shrinkage was also measured by Zhang et al. (2009) and Weimann and Li (2003). Weimann and Li (2003) conducted free drying shrinkage tests and restrained drying ring

tests. The tests showed ECC to have high free drying shrinkage but under restrained conditions ECC had tight crack widths of 30-50 μm. Since the durability is more dependent on the crack width than free drying shrinkage, ECC should be more durable than concrete. Zhang et al. (2009) tested a newly developed low drying shrinkage cementitious composite. The new composite was able to reduce the drying shrinkage by almost 700% and maintain the unique strain-hardening and multiple cracking performances. The composite has a strain capacity of approximately 2.5% and a tensile strength of 4-5 MPa. The testing proved that ECC can be made to have low drying shrinkage, and thus prevent early age shrinkage induced cracking.

2.3 Durability Testing Methods

Test methods used to monitor the durability of HES-ECC for this research include ASTM C157, ASTM C666, and two non-standardized tested that measured the semi-adiabatic temperature rise and autogenous shrinkage of the HES-ECC.

2.3.1 ASTM C157: Length Change of Hardened Hydraulic Cement Mortar and Concrete

ASTM C157 standard *Length Change of Hardened Hydraulic-Cement Mortar and Concrete* measures length change of mortar or concrete due to causes other than applied force and temperature change, specifically, drying shrinkage. This test quantifies potential volumetric changes due to expansion or contraction of the concrete and is useful for comparative evaluation of different hydraulic cement concrete mixtures.

The procedure for this standard consists of casting at least three rectangular prism specimens with gage studs on each end of the specimen. The concrete prisms are cast in two approximately equal layers and consolidated by rodding or vibrating each layer. After 24 hours of curing the specimens are de-molded and placed in lime-saturated water maintained at 73 ± 1^{o}F for

at least 30 minutes before an initial comparator reading is taken. This minimizes error in the length measurement due to temperature variations. The length change of the specimen is computed by taking the difference between the comparator reading and the reference bar and then dividing by gage length. The specimens are then cured in lime-saturated water for 28 days and another comparator reading is taken. For the remainder of the testing period specimens are stored in a drying room at a temperature of 73 ± 3°F with a relative humidity of 50 ± 4%. After final curing, comparator readings for the specimens are taken at 4, 7, 14, and 28 days and after 8, 16, 32, and 64 weeks (ASTM, 2017).

2.3.2 ASTM C666: Resistance of Concrete to Rapid Freezing and Thawing

ASTM C666 *Resistance of Concrete to Rapid Freezing and Thawing* follows one of two procedures that are intended to determine the effects of freezing and thawing cycles on the properties of concrete. The specimens are continually immersed in water for Procedure A. Procedure B the specimens are frozen in air and then thawed in water. Procedure B more realistically simulates the patterns that occur in the field while Procedure A is a more conservative approach because the specimens are saturated for the duration of testing. A freezing-and-thawing cycle occurs over a 2-5 hour period where the temperature is lowered from 40 to 0 °F and then raised back to 40 °F. Prior to beginning freeze-thaw cycles, the specimens are kept in lime saturated water for 14 days. Initial readings of the mass, resonant frequency of vibration, and length change are recorded for each concrete specimen. Readings are then taken at intervals not exceeding 36 cycles. Based off of the collected data, an RDME value and the percent expansion is determined. The experiment ends when one of the following occurs: the specimens undergoes 300 freeze-thaw cycles, the RDME reaches 60% of the initial modulus, or the specimens reach a 0.10% expansion (ASTM, 2015).

2.3.3 Semi-adiabatic Temperature Rise Test

The semi-adiabatic temperature rise test measures the temperature of a hydrating concrete cylinder and temperature of the insulated atmosphere around the cylinder. By measuring the

temperature of the cylinder, it can be determined if the cylinder will reach temperatures that could cause delayed ettringite formation (DEF) which occurs when temperatures reach above 70-80 ^{o}C at an early age (Lim et al., 2016)

The procedure for this test consists of casting a 6" x 12" cylinder with a thermocouple embedded at the center of the specimen. The concrete was placed in three layers and rodded 25 times at each layer. After casting the specimen, it was placed in an insulated barrel and the thermocouple was attached to a thermocouple data logger. The temperature was measured in three places: the center of the concrete cylinder, just outside of the concrete cylinder, and at the edge of the insulated barrel. The data was logged for 2-3 days. Based upon the data, a curve of the temperature versus time was graphed. Numerical analysis of the data allowed for predictions of the concrete adiabatic temperature rise characteristics.

2.3.4 Autogenous Shrinkage Test

The autogenous shrinkage test attempts to measure the length change of concrete due to the formation of new products during cement hydration. This test followed the procedure by Cusson (2008) that uses sealed prisms to measure the autogenous shrinkage. This test is conducted by casting the concrete in rectangular prisms with steel rods protruding from each end. A washer is welded to the end of the steel rod that is cast into the concrete so that the rod moves with the concrete as it changes length without puncturing the concrete. After casting, the prisms are placed on a steel frame that holds the linear variable differential transformers (LVDTs). The LVDTs measure the length change of the prisms. The data was collected at varying intervals up to 9 days. The frequency and duration of data collection can vary depending on the desired work.

2.4 Summary

Engineered cementitious composites are a fiber reinforced concrete that are characterized by their ductility and multiple tight width cracks upon loading. This literature review discussed

the development and design basis for ECC. Then reviewed high early strength ECC and how the micromechanical design model applies to these types of mixtures. The review then shifted to a discussion of the durability of ECC under mechanical, chemical, and thermal loading. Finally, an overview of the durability test methods used for this research was presented.

Chapter 3 – Materials

This chapter summarizes the materials used in this study. The materials include aggregates, Polyvinyl Alcohol (PVA) fibers, Type III portland cement, metakaolin, a blended cement with Type III portland cement and calcium sulfo-aluminate (CSA) cement and various admixtures.

3.1 Aggregates

The only aggregate used for this research was fine aggregates. The fine aggregate was naturally occurring river sand. The absence of coarse aggregates in HES-ECC is due to the increase in matrix stiffness when coarse aggregate is present. This leads to a loss in ductility because of delayed crack initiation which prevents steady-state flat-crack propagation (Sahmaran et al., 2012). All aggregates were oven dried before mixing. The absorption capacity and specific gravity of the aggregates were 0.57% and 2.6, respectively.

Figure 3-1: Fine Aggregate – River Sand

3.2 Cements and Supplementary Cementitious Materials

Type III portland cement and a blended Type III portland and calcium sulfo-aluminate cement were used in this study. Metakaolin provided by BASF was used as a partial replacement for Type III portland cement for certain mixtures. Table 3-1 shows the mill test results for Monarch Type III portland Cement and Table 3-2 provides the Physical properties of MetaMax® metakaolin.

Table 3-1: Mill Test Results for Monarch Type III portland Cement

Property		Reported Value	Spec Limit
Physical Properties			
325 Sieve, % Passing		99.7	-
Blaine fineness, specific surface – Air Permeability (cm^2/g)		5,860	-
Time of Setting, Gilmore Test:	Initial (hrs:min)	1:40	60 min
	Final (hrs:min)	2:35	600 max
Air Content of Mortar (volume %)		7.0	12.0 max
Autoclave Expansion (%)		-0.014	0.80 max
Compressive Strength (psi)	1 Day	3,709	1,740 min
	3 Days	5,019	3,480 min
	7 Days	5,564	-
Chemical Properties			
SiO_2 – Silicon Dioxide (%)		21.20	-
Fe_2O_3 – Ferric Oxide (%)		2.89	6.0 max
Al_2O_3 – Aluminum Oxide (%)		4.06	6.0 max
CaO – Calcium Oxide (%)		64.15	-
MgO – Magnesium Oxide (%)		1.53	6.0 max
SO_3 – Sulphur Trioxide (%)		2.79	3.5 max
Loss on Ignition (%)		0.85	3.0 max
Insoluble Residue (%)		0.22	1.50 max
Free Lime (%)		1.29	-
Na_2O – Sodium Oxide (%)		0.17	-
K_2O – Potassium Oxide (%)		0.53	-
Equivalent Alkalies (%)		0.51	0.60 max
Potential Calculated Compounds			
C_3S – Tricalcium Silicate (%)		60.7	-
C_2S – Dicalcium Silicate (%)		15.0	-
C_3A – Tricalcium aluminate (%)		5.9	8 max
C_4AF – Tetracalcium aluminoferrite (%)		8.8	-

Table 3-2: Physical properties of MetaMax® metakaolin provided by BASF

Physical Properties	Typical Value
Physical Form	Highly Pulverized Powder
Special Modifications	Dehydroxylated
GE Brightness (%)	85
Screen Residue, 325 Mesh (%)	0.05
Free Moisture (%) measured at 105ºC	0.5
pH (20% solids)	6
Median Particle Size, Sedigraph (μm)	1.3
Specific Gravity (g/cm^3)	2.50
Bulk Density, Loose lb/ft^3 (kg/m^3)	16 / 260
Bulk Density, Tamped lb/ft^3 (kg/m^3)	30 / 480

3.3 Polyvinyl Alcohol (PVA) Fibers

The fibers used for the research were RECS15 by Nycon are 8 denier, ductile mono-filament PVA fibers. Table 3-3 summarizes the specifications of the fibers. Figure 3-2 depicts the PVA fibers.

Table 3-3: Properties of RECS15 mono-filament PVA fibers.

Configuration	Monofilament
Tensile Strength	240 ksi (1600 MPa)
Flexural Strength	5700 ksi (40 GPa)
Filament Diameter	8 Denier (38 microns)
Available Lengths	0.375”(8mm)
Aspect-Ratio	210.52
Melting Point	435º F (225º C)
Water Absorbtion	<1% by Weight
Color	White
Elongation	6%
ZrO_2 Content	NA

Figure 3-2: Polyvinyl Alcohol Fibers

3.4 Water Reducer

ADVA® 140M from GCP Applied Technologies and EUCLID® Plastol 6400 type A/F water reducer were the water reducers used for HES-ECC mixtures in this study. The addition range for ADVA® 140M can range from 2–20 oz/cwt of cement. The typical addition rates for high-range water reducers is 9–16 oz/cwt of cement (Gcp, 2020). The recommend dosage for EUCLID® Plastol 6400 is 3–12 oz/cwt of cement (Euclid, 2020). Both admixtures are Polycarboxalate based and conceptually interchangeable, but with different dosage rates. Therefore, they were able to be used interchangeably with little influence on the scope of this research.

3.5 Accelerator

Calcium chloride was used as an accelerator for all concrete mixtures in this study except for the mixtures containing the Type III/CSA blended cement. The Type III/CSA Cement does not require acceleration for high early strength due to the rapid hydration of the CSA.

Chapter 4 - Methodology

This chapter describes the methodology for mixing, standardized testing, and other durability testing.

4.1 Concrete Mixture Proportioning

The mixture design for HES-ECC was based on research previously conducted by Wang and Li, 2006. Their mixtures used a water-to-binder (w/b) ratio of around 0.33 and a fiber volume fraction of 2%. The mixtures in this study used a w/b ratio of 0.34 for three mixtures and 0.4 for one mixture. Table 4-1 outlines the material mixture composition and proportion.

Table 4-1: Mixture Proportions

ID	Cement (lb/yd^3)	Metakaolin (lb/yd^3)	Sand (lb/yd^3)	Water (lb/yd^3)	PVA Fibers, V_f, (lb/yd^3)	HRWR (oz/cwt)	CaCl (oz/cwt)
CEM III	1620	-	1620	544.3	32.4	17.6	38.4
CSA/III	1620	-	1620	544.3	32.4	17.6*	-
MK8%	1523	89	1612	548.2	32.2	20.0*	38.4
MK15%	1368	150	1518	607.0	30.4	20.0*	38.4

*High range water reducer (HRWR) was added to each mixture as needed.

The mixtures was prepared in either a Lancaster Counter-Current mixer with 1.5 cu. ft. capacity or in a Mud Hog mixer according to the following mixture procedure:

1. Mix dry ingredients (cement, metakaolin, and silica sand) for approximately 1 minute;
2. Slowly add water and continue mixing for 1 to 2 minutes;
3. Add HRWRA (when needed); continue mixing for 1 to 2 minutes until a consistent mixture is reached;
4. Slowly add PVA fibers and mix for 2 minutes until fibers are well-distributed;

5. Add accelerating admixture (when needed) and mix for 1 minute before casting into molds.

The entire mixing procedure took between 5 to 12 minutes for each mixture. Specimens were cast according to ASTM C192 and were placed in the moist room within 24 hours of casting. All specimens were cured in the moist room until testing. The mixers are shown in Figure 4-1 and Figure 4-2.

Figure 4-1: Lancaster Counter-Current Mixer

Figure 4-2: Mud Hog Mixer

4.2 Laboratory Testing

The main objective of this study was to test the durability of HES-ECC and contribute to a growing body of work on HES-ECC. Early age strengths of the four mixtures were tested to ensure that it reached minimum strength criteria desired for common applications of high early strength concrete. These requirements vary depending on the transportation agency or specific application, but are typically in the range of 1000 to 3000 psi for compressive strength and between 350 to 500 psi for flexural strength (Wang and Li, 2006). The research addressed durability problems that are caused by drying shrinkage, autogenous shrinkage, high temperatures during cement hydration, and freezing-and-thawing cycles.

4.2.1 Strength Testing

Compression and split tensile test were conducted at 4, 6, and 24 hours for each mixtures according to ASTM C39 and ASTM C496. For both tests four 4” by 8” cylinders were prepared to be tested at the appropriate age. After casting the specimens, they were placed in the curing room, de-molded at approximately four hours, and then stored until testing at the specified age. Figure 4-3 and Figure 4-4 depict the Forney compression machine and the compression machine used for split tensile testing.

Figure 4-3: Forney Compression Machine

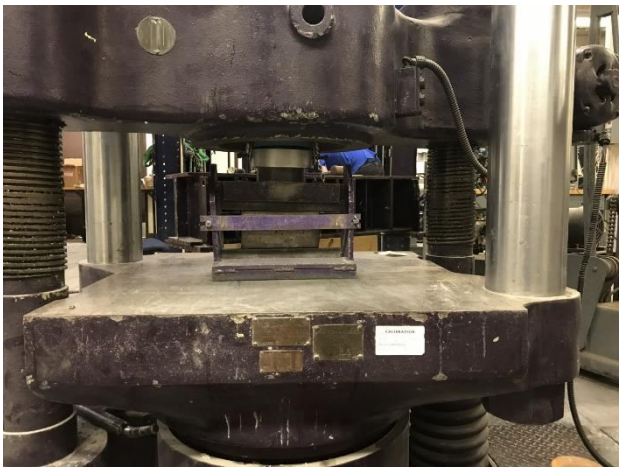

Figure 4-4: ASTM C496 Split Tensile Strength Test

4.2.2 Autogenous Shrinkage

Standardized tests such as ASTM C1698 and ASTM C1581 describe methods of measuring autogenous shrinkage of cements, mortars, and concretes. ASTM C1698 is a standardized test method that measures autogenous shrinkage by periodically assessing the deformation of mortar or cements poured in a corrugated polymeric tube. ASTM C1581 uses a steel ring and strain gauges to measure the autogenous shrinkage if the concrete is sealed. However, other researchers have

developed non-standardized test methods to measure autogenous shrinkage in concrete that include cylinders (Craeye & De Schutter, 2008), sealed prisms (Cusson, 2008; Weiss et al., 1999), and large corrugated tubes (Tian & Jensen, 2008). This study followed the method by Cusson (2008) that uses the sealed prisms.

Three 3" by 4" by 16" prisms were made for each mixture. The prisms were set on a steel frame and aligned such that linear variable differential transformers (LVDTs) could be connected at each end of the specimen. At both ends of each specimens neoprene pads were installed to allow for expansion of the HES-ECC at an early age. All specimens were covered with a plastic sheet to seal the prisms. To allow for free movement during shrinkage lubrication oil was applied to the sides of the prisms. Figure 4-5 shows the set-up used to measure the autogenous shrinkage of HES-ECC prisms.

Figure 4-5: Prisms Measuring Autogenous Shrinkage

4.2.3 Drying Shrinkage

Following ASTM C157 the long-term drying shrinkage was measured for each mixture. After casting three 3" by 4" by 16" the specimens were covered with plastic and then de-molded at approximately four hours. An initial reading was taken and then the specimens were placed in lime saturated water for 28 days. After the 28 days, another reading was taken and the prisms were

stored in a drying room at a temperature of 73 ± 3ºF with a relative humidity of 50 ± 4%. The length change comparator is shown in Figure 4-6

Figure 4-6: Length-Change Comparator (ASTM C157)

4.2.4 Freezing and Thawing

This study followed ASTM C666 Procedure B to measure the freeze-thaw (F/T) durability of each HES-ECC mixture. For each mixture three 3" by 4" by 16" specimens were cast, and then covered with plastic until being de-molded at approximately four hours. After de-molding the specimens were placed in lime saturated water for 14 days. Then initial readings of mass, resonant frequency of vibration, and length change were taken and the specimens were placed in the Scientemp F/T machine (Figure 4-7) which is programmed to run eight cycles every day. Readings were then taken at intervals not exceeding 36 cycles until each specimen had undergone at least

300 cycles, the RDME reaches 60% of the initial modulus, or the specimens reach a 0.10% expansion.

Figure 4-7: ScienTemp F/T Machine (ASTM C157)

4.2.5 Semi-adiabatic Temperature Rise

The semi-adiabatic temperature rise was measured by casting a 6” x 12” cylinder with a thermocouple embedded at the center of the specimen. Once the specimen was cast it was immediately placed in an insulated barrel and the thermocouple was attached to a thermocouple data logger. The temperature was measured in three places: the center of the concrete cylinder, just outside of the concrete cylinder, and at the edge of the insulated barrel. The data were logged for three to five days. Figure 4-8 depicts the insulated barrel used while measurements were taken of the temperature change of the HES-ECC.

Figure 4-8: Insulated Barrel with HES-ECC Cylinder

Chapter 5 - Results

High-performance concrete is defined as a concrete that has superior mechanical and durability properties than that of normal concrete. For a concrete to be durable it must be able resist deterioration despite the exposure conditions and thus maintain serviceability throughout the service life (Neville, 1996). The durability of concrete can be measured by a variety of methods since deterioration of concrete can be caused by a variety of factors. This research study conducted strength tests measuring the compressive and tensile strength evolution at an early age. The heat generation during hydration was measured by a semi-adiabatic temperature rise test. The durability was tested by measuring the drying shrinkage, autogenous shrinkage, and freezing-and-thawing cycles.

5.1 Compressive Strength Testing

Compressive strength test results are illustrated in Figure 5-1 for all mixtures. The compressive strength was measured using an automated variable frequency drive Forney testing machine. Compressive strength was test at 4, 6, and 24 hours. End caps with neoprene pads were placed on each cylinder to prevent eccentric axial loading during testing. The ramping rate was 35±7 psi/sec. Target range for compressive strength was between 1000 to 3000 psi within four to six hours.

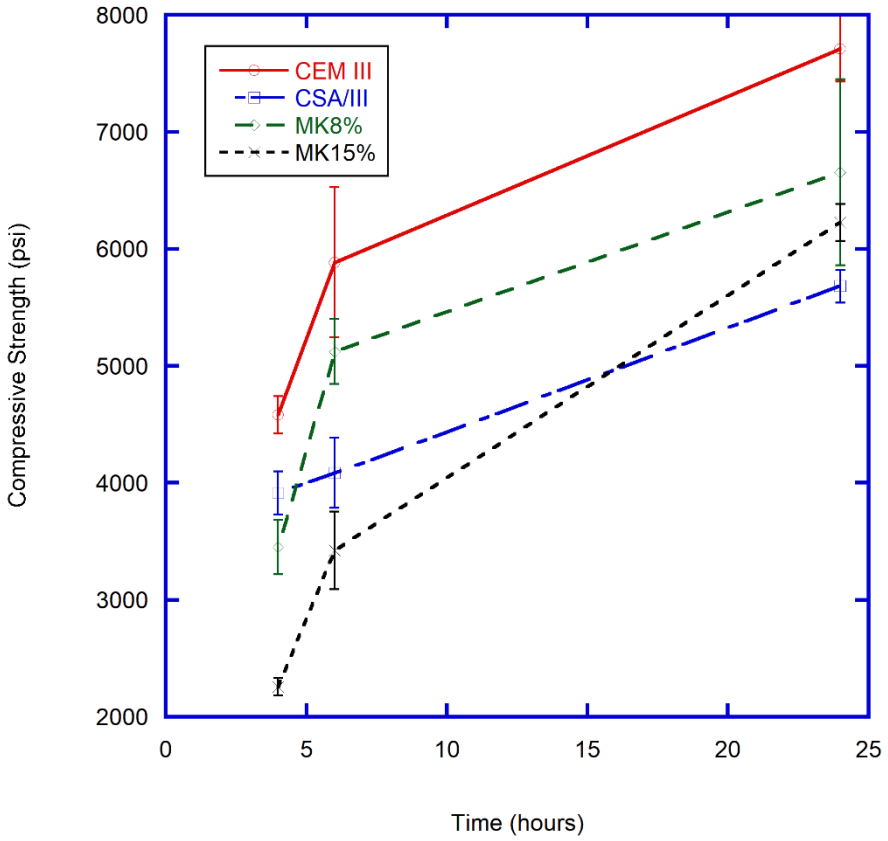

Figure 5-1: Average Compressive Strength of All Mixtures

5.2 Split Tensile Strength Testing

A graphical representation of the split tensile strength test results are provided in Figure 5-2. Split tensile tests were conducted at 4, 6, and 24 hours on a hydraulic compression machine. The rate of loading was within a range of 100 to 200 psi/min. An 1/8" wooden bearing strip was placed at the top and bottom of the cylinder before testing. Target range for split tensile strength was between 350 to 500 psi within four to six hours.

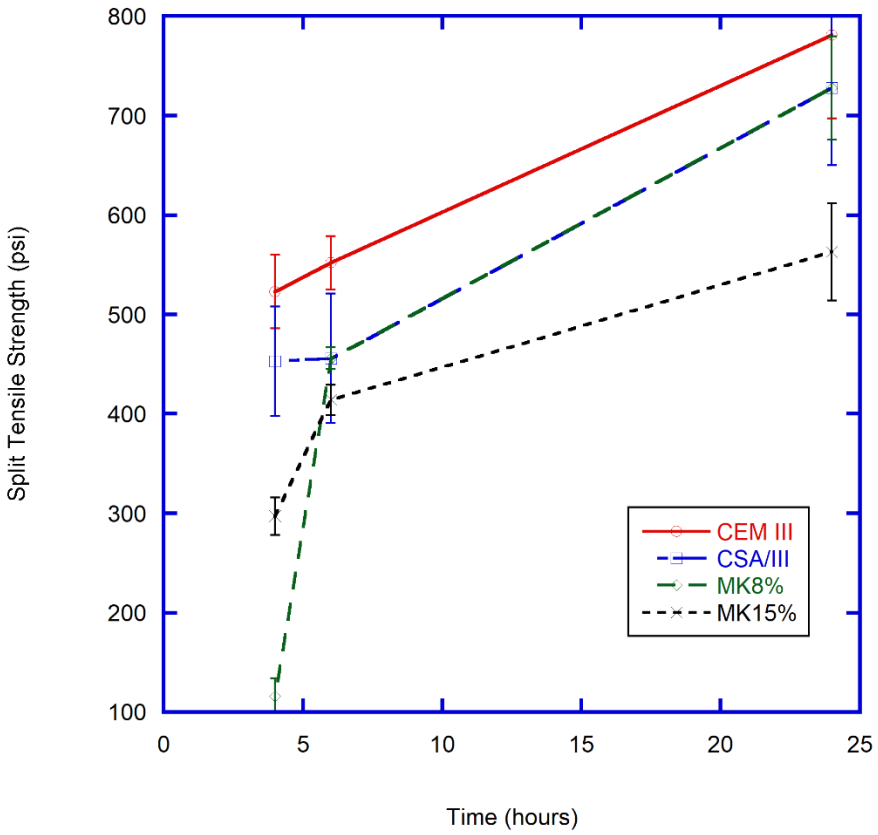

Figure 5-2: Average Split Tensile Strength of All Mixtures

5.3 Split Tensile Strength Versus Compressive Strength

The relationship between Split tensile strength and compressive strength had been represented using a variety of expressions. Equation 5-1 shows the expression used for the lower bound based off the ACI building code. An upper bound equation was developed by ACI committee 363 and is expressed in Equation 5-2 (Ahmad, and Shah, 1985). Ahmad and Shah, 1985 developed an equation to better represents the data and is shown in Equation 5-3. Figure 5-3 illustrates the average split tensile strength versus compressive strength and shows the representative expressions that relate the split tensile strength to the compressive strength.

$$f_{st} = 6\left[f'_c\right]^{0.5} \quad (5\text{-}1)$$

$$f_{st} = 7.4\left[f'_c\right]^{0.5} \quad (5\text{-}2)$$

$$f_{st} = 4.34\left[f'_c\right]^{0.55} \quad (5\text{-}3)$$

where,

$f_{st} = splitting\ tensile\ strength, psi;$

$f'_c = compressive\ strength, psi$

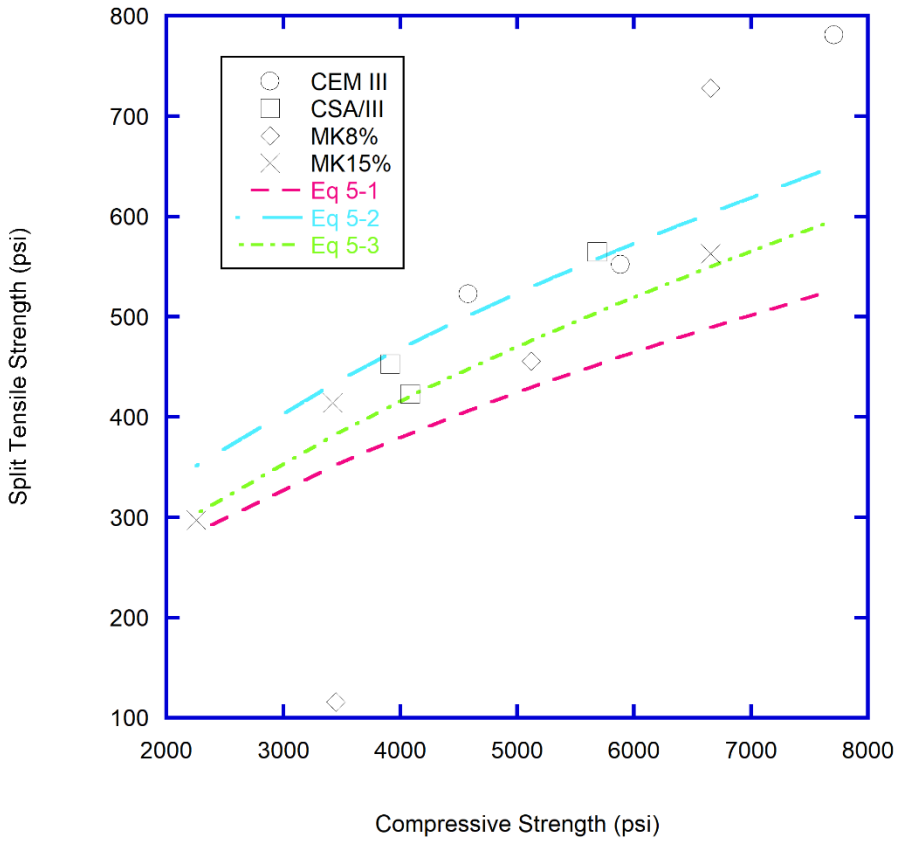

Figure 5-3: Average Split Tensile Strength Versus Average Compressive Strength

5.4 Dry Shrinkage Testing

Drying shrinkage measurements were made at 3, 7, 14, and 28 days and 8, 10, 16, and 32 weeks. Figure 5-4 illustrates the results from the drying shrinkage test. Equation 5-4 was used to calculate the percentage of length change caused by drying shrinkage.

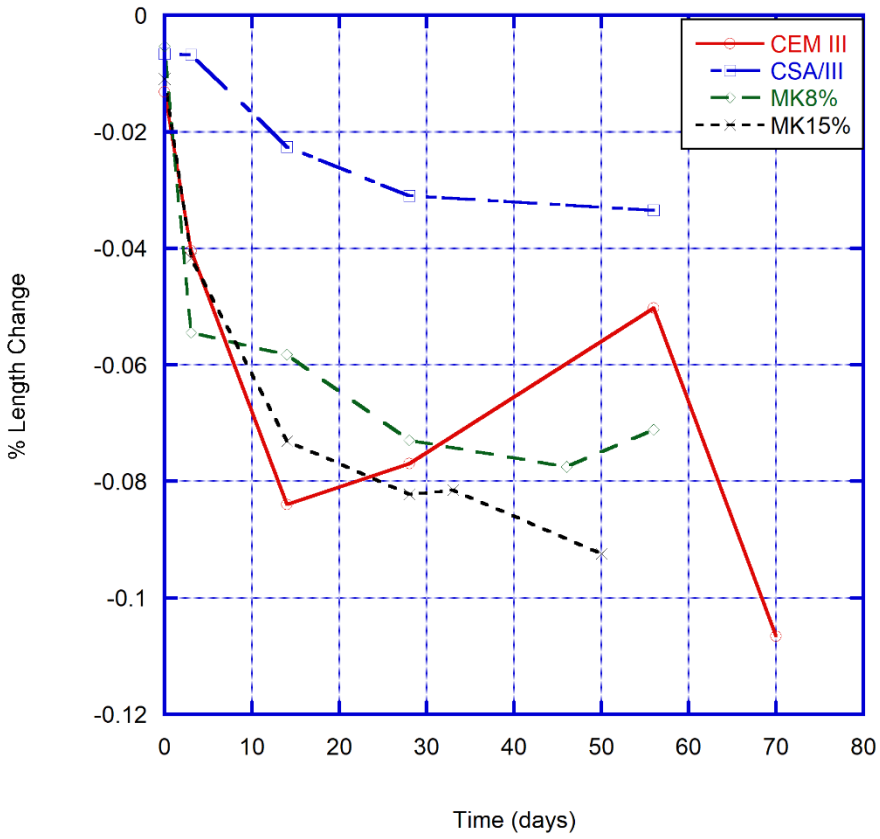

Figure 5-4: Drying Shrinkage Measurements of All Mixtures

$$\Delta L_x = \frac{CRD - intial\ CRD}{G} x100 \quad (5\text{-}4)$$

where,

$\Delta L_x = length\ change\ of\ specimen\ at\ any\ age, \%$;

CRD $= difference\ between\ comparator\ reading\ of\ the\ specimen\ and\ the\ reference\ bar\ at\ any\ age$;

and

$G = the\ gage\ length$ (16 $inches$ [400 mm])

5.5 Autogenous Shrinkage Testing

Autogenous shrinkage measurements were taken for up to nine days at various time intervals. Figure 5-5 illustrates the results from the autogenous shrinkage test. Equation 5-5 was used to calculate the percentage of length change caused by autogenous shrinkage.

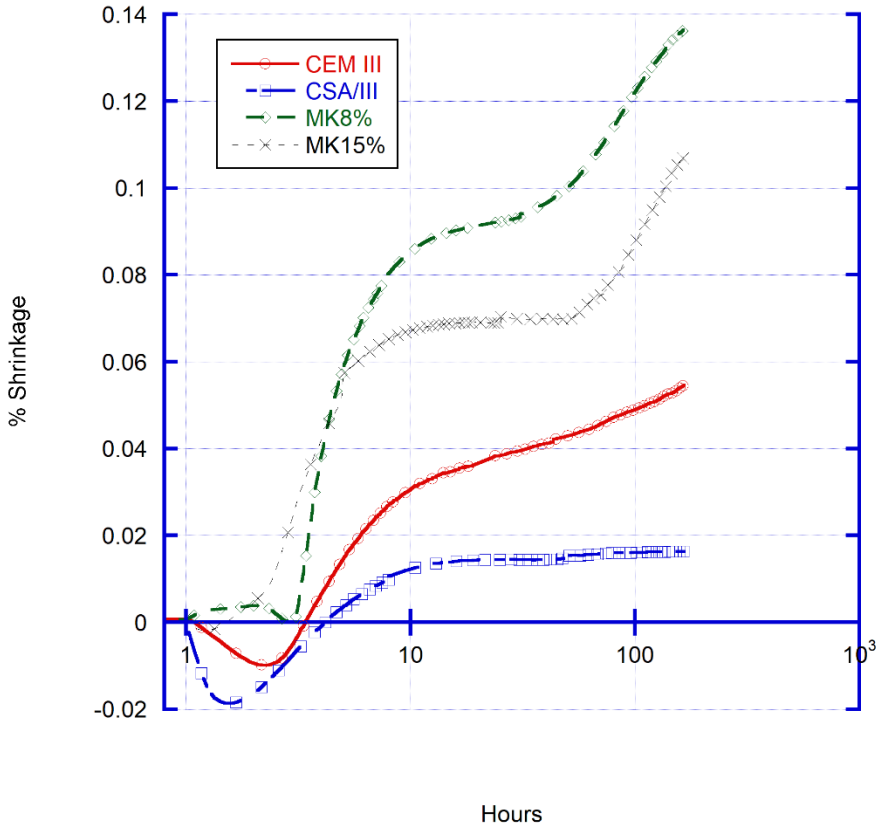

Figure 5-5: Autogenous Shrinkage Measurements

$$\Delta L_x = \frac{\pm L}{G} x100 \qquad (5\text{-}5)$$

where,

$\Delta L_x = length\ change\ of\ specimen\ at\ any\ age, \%$;

$\pm L = expansion\ or\ contraction\ at\ any\ age$;

and

$G = fixed\ distance\ between\ sawed\ studs\ in\ the\ specimen$

5.6 Freeze-Thaw Testing

The changes in mass, length change, and RDME of specimens were measured for all mixtures as part of the freeze-thaw testing. The results from testing were graphed and are discussed in the following subsections.

5.6.1 Change in Mass

The mass was measured and recorded at intervals of approximately 36 cycles. A graphical representation of the mass change is shown in Figure 5-6. Mass change was calculated using Equation 5-6.

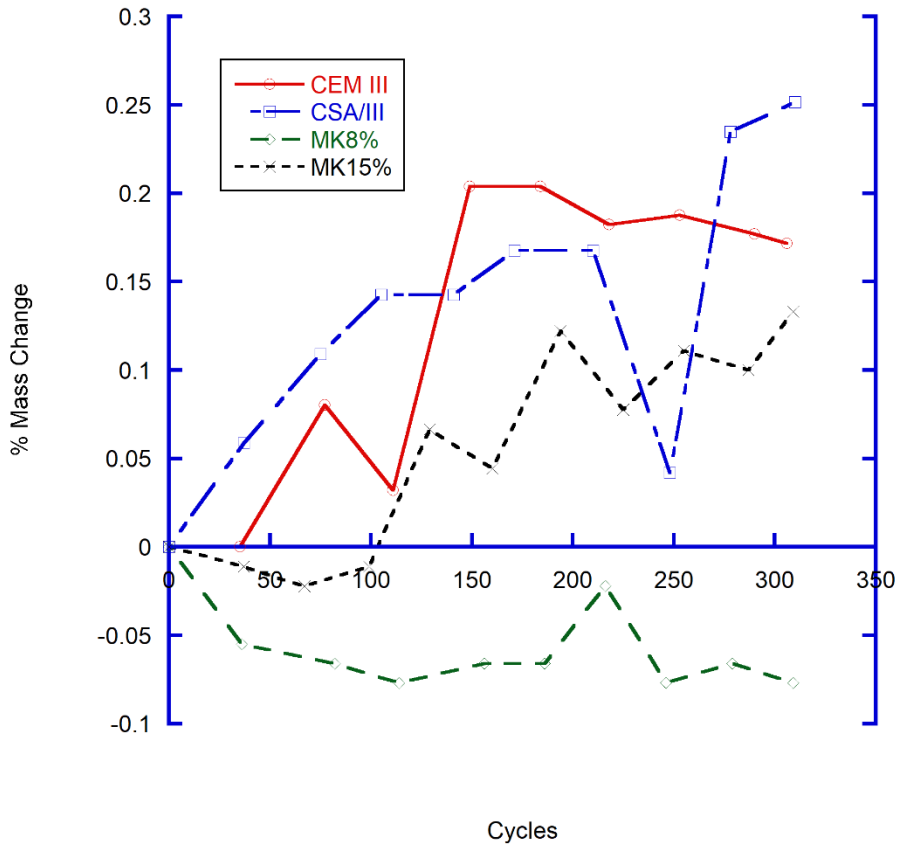

Figure 5-6: Mass Change Measurements of All Mixtures

$$\text{Mass Change (\%)} = \frac{(m_x - m_o)}{(m_o)} x100 \quad (5\text{-}6)$$

where,

$m_x = mass\ reading\ at\ x\ freeze - thaw\ cycles, lb;$

$m_o = intial\ mass\ reading, lb;$

5.6.2 Length Change

The length change was measured and recorded at intervals of approximately 36 cycles. Figure 5-7 shows a graphical representation of the length change data.

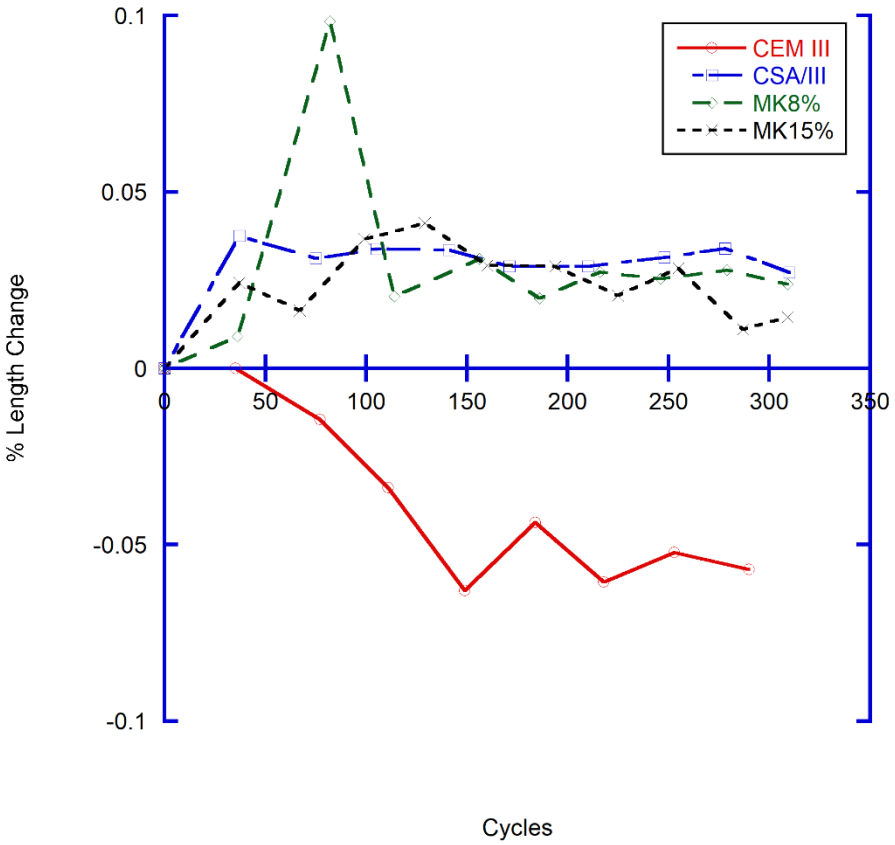

Figure 5-7: Length Change Measurements of All Mixtures

5.6.3 Relative Dynamic Modulus of Elasticity (RDME)

The RDME change was measured and recorded at intervals of approximately 36 cycles. Figure 5-8 shows a graphical representation of the freeze-thaw data. Computation for RDME were made according to Equation 5-7.

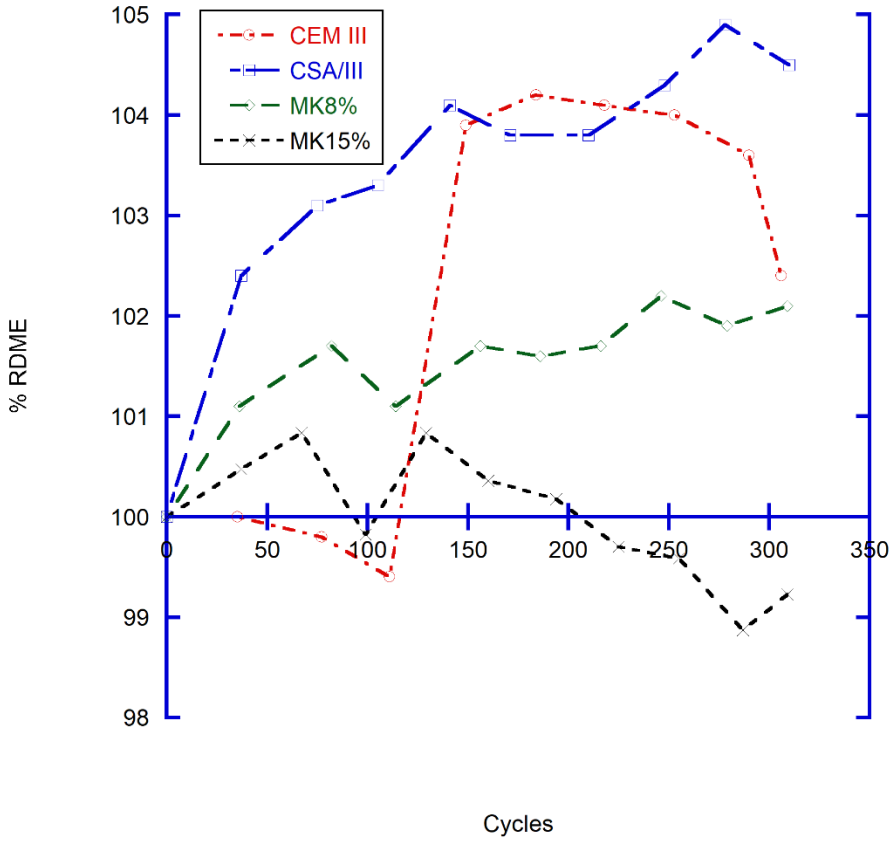

Figure 5-8: RDME Measurements of All Mixtures

$$\text{RDME } (\%) = \frac{(E_x)}{(E_o)} x100 \quad (5\text{-}7)$$

where,

$E_x = modulus\ reading\ at\ x\ freeze - thaw\ cycles, GPa;$

$E_o = intial\ modulus\ reading, GPa;$

5.7 Semi-adiabatic Temperature Rise

The heat generation from all mixtures was measured and is shown graphically in Figure 5-9.

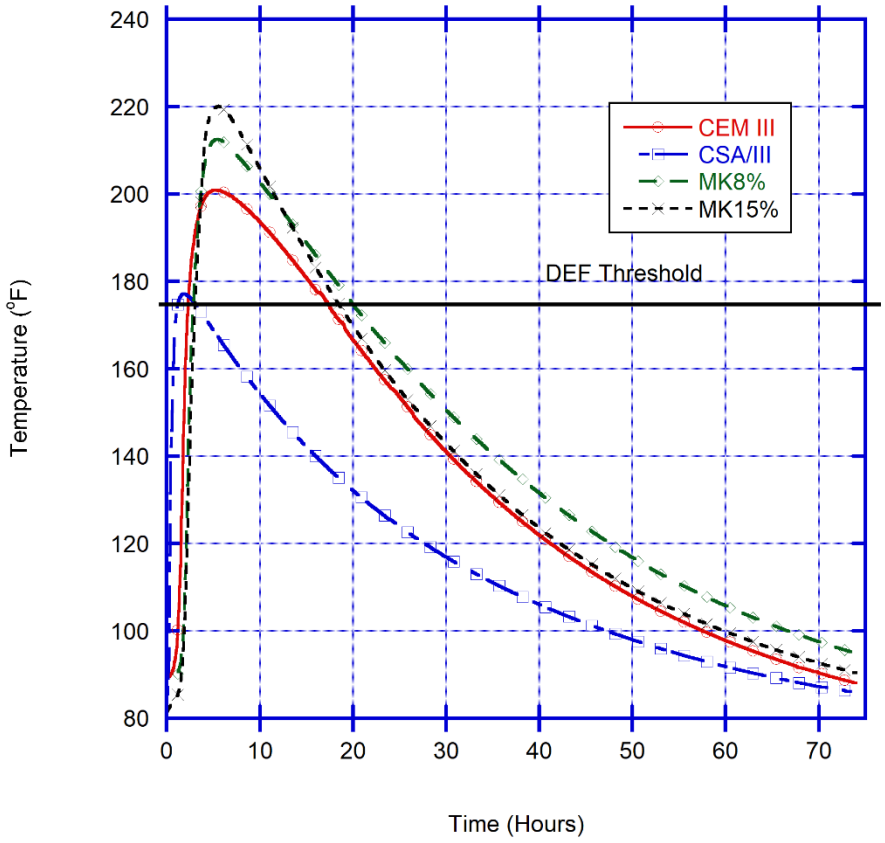

Figure 5-9: Temperature Rise Measurements for All Mixtures

Chapter 6 - Analysis and Discussion

This section analyzes and provides discussions on the results of the strength testing, shrinkage testing, freeze-thaw testing, and semi-adiabatic temperature rise testing.

6.1 Strength Behavior

A target range for minimum strength requirements was set based off common requirements set by transportation agencies. The target range for compressive strength was set to 1000 to 3000 psi and split tensile strength/flexural strength was set to a range of 350 to 500 psi. All mixtures were within the compressive strength range or above within four hours. CEM III performed the best with compressive strengths above 4500 psi at four hours and above 7700 psi at 24 hours. Similarly, the split tensile strength of all mixtures was within or above the range at 6 hours. MK8% and MK15% were slower to develop split tensile strength and were not within range after 4 hours. Equation 5-2 developed by ACI committee 363 most accurately predicts the split tensile strength based off of the compressive strength for the data. However, without more data it is difficult to determine unequivocally how accurate the expressions predicts the split tensile strength for HES-ECC.

6.2 Autogenous Shrinkage

MK8% had the highest autogenous shrinkage of almost 0.14% followed by MK8% which had a shrinkage of over 0.1% after seven days. The autogenous shrinkage of MK15% is lower than MK8% due to the mixture being designed with a w/cm ratio of 0.4. CEM III had a shrinkage of over 0.05% after seven days. CSA/III shrank approximately 0.0165% at seven days. CSA in the CSA/III blend is why there is relatively less shrinkage than the other mixtures.

6.3 Drying Shrinkage

Due to high amounts of cement and no coarse aggregate in HES-ECC, all mixtures showed high percentage of drying shrinkage. The data shows that CEM III expands between the 28 day test

and eight and ten week tests. The mechanisms causing the expansion of the concrete are unclear. MK15% had a higher amount of drying shrinkage than MK8% despite having a lower autogenous shrinkage this is due to the higher w/cm ratio of MK15%. CEM III at 10 weeks shrank more than 0.10% due to drying. CSA/III had the least amount of shrinkage at 28 days.

6.4 Freeze/Thaw Durability

All mixtures experienced a percentage increase of mass, except for MK8% which had a slight loss of mass. CSA/III had highest mass increase of 0.25% after 310 cycles. CEM III was the only mixture to shrink during the freeze-thaw cycles while MK15% had the highest expansion around 0.05%. All mixtures showed an increase in RDME. CEM III showed a reduction in RDME, but after an extended hydration period due to machine maintenance the RDME increased. However, it showed a decrease after the increase in RDME.

6.5 Semi-adiabatic Temperature Rise

All mixtures reached temperatures above 176 ^{o}F. This is concerning because deterioration from delayed ettringite formation can occur when temperatures in concrete reach 158-176 °F due to early-age heat release during hydration. MK8% reached temperatures of over 212 ^{o}F which was higher than CEM III which peaked at approximately 201 ^{o}F. MK15% reach the highest temperature above 212 ^{o}F. CSA/III was above 176 ^{o}F for the least amount time at approximately an hour and half.

Chapter 7 - Conclusions

Due to environmental and mechanical loading concrete structures deteriorate during the service life leading to premature failure of the structure. Concrete repairs are required throughout the service life of a concrete structure for the structure to remain in service. Additionally, concrete structures that need to be reopened quickly require a fast hardening concrete. A material such as HES-ECC is able to develop strength quickly and maintain durability due to their ability to maintain tight crack widths upon loading which minimizes the intrusion of unwanted substances, high ductility/deformation compatibility with concrete substrate structure, and high-fracture toughness which allows it to defuse and arrest unstable crack propagation. For these reasons it is thought that HES-ECC will be a high performing and effective repair material. In this study, the deterioration of HES-ECC was evaluated by conducting various concrete testing methods. Early strength evolution and heat generation of the four HES-ECC mixtures was also measured. The following was concluded from this research:

- For most applications where high early strength concrete is needed the minimum strength requirements were met. All mixtures had a compressive strength of at least 2200 psi within four hours and a split tensile strength of over 400 psi at six hours. The target range for compressive strength and split tensile strength based upon requirements from different transportation agency was 1000 to 3000 psi and 350 to 500 psi, respectively.
- All mixtures demonstrated a high amount of drying shrinkage due to the high amount of cement, and no coarse aggregate in the mixtures. After 10 weeks of drying shrinkage, the shrinkage for CEM III was more than 0.10%.
- Since ASTM C157 is not able to capture early-age shrinkage behavior, a laboratory made apparatus with sufficient sensitivity to measure early age shrinkage due to chemical shrinkage was used for all mixtures. This early autogenous shrinkage behavior may be an indicator of future durability problems for the concrete since early age shrinkage can cause stress gradients which may cause cracking and ultimately deterioration of the concrete.

- CSA/III had lower early age shrinkage and drying shrinkage due to the presence of CSA. CSA expands due to the formation of ettringite and amorphous phases.
- All mixtures had negligible deterioration after more than 300 freeze-thaw cycles. After 300 cycles, mixtures had a slight reduction in mass while some even showed a slight increase in mass. MK15% had the highest expansion of 0.05%. The only mixture to shrink was CEM III with a shrinkage around 0.01%.
- All mixtures increased in RDME throughout the freeze-thaws cycles except CEM III. CEM III showed a decrease in RDME and then a positive jump in RDME due to an extended hydration period during machine maintenance. Overall, all of these mixtures seem to be resistant to freeze-thaw deterioration. This could be from the extra air that is entrapped during mixing due to the presence of fibers and no coarse aggregate in the mixture.
- All mixtures demonstrated rapid heat generation which led to high specimen temperature. This is likely due to the high cement content and finer cement particles of Type III cement. CEM III, MK8%, and MK15% reached temperatures above 176 ^{o}F for at least 14 hours. CSA/III was above 176 ^{o}F for approximately an hour and half. Temperatures above 176 ^{o}F could lead to delayed ettringite formation which may cause deterioration of the concrete.

Future work includes evaluation of HES-ECC due to other mechanisms of deterioration. This would include further research into DEF, specifically how it affects the durability of HES-ECC. Also, conducting work on how susceptible HES-ECC are to alkali-silica reaction. Alkali-silica reaction occurs between highly alkaline cement and reactive silica found in common aggregates and forms an expansive chemical product creates pressure inside the aggregate. If the pressure exceeds the strength of the matrix then spalling and eventually failure of the matrix can occur. This is especially a concern in HES-ECC due to the high cement content.

Bibliography

Ahmad, S. H., and Shah, S.P., 1985 "Structural Properties of High Strength Concrete and Its Implications for Precast Prestressed Concrete," PCI Journal, V. 30, No. 6, pp. 92-110.

ASCE. 2017, "Report Card for America's Infrastructure," http:// www.infrastructurereportcard.org/. (accessed October 5, 2020).

ASTM. 2017, ASTM C496: Splitting Tensile Strength of cylindrical Concrete Specimens. In *Annual Book of ASTM Standards.* West Conshohocken, PA.

ASTM. 2017, ASTM C157: Length Change of Hardened Hydraulic-Cement Mortar and Concrete. In *Annual Book of ASTM Standards.* West Conshohocken. PA.

ASTM. 2015, ASTM C666: Resistance of Concrete to Rapid Freezing and Thawing. In *Annual Book of ASTM Standards.* West Conshohocken, PA.

ASTM. 2020, ASTM C39: Comprssive Strength of Cylindrical Concrete Specimens. In *Annual Book of ASTM Standards.* West Conshohocken, PA.

ASTM. 2019, ASTM C192: Making and Curing Concrete Test Specimens in the Laboratory. In *Annual Book of ASTM Standards.* West Conshohocken, PA.

Bazant, Z. P., and Najjar, L. J., 1971, "Drying of concrete as a nonlinear diffusion problem," Cement and Concrete Research, V. 1, pp. 461–473.

Bentz, D. P., and Peltz, M. A., 2008, "Reducing Thermal and Autogeneous Shrinkage Contributions to Early-Age Cracking," ACI Materials Journal, V. 105, No. 4, pp. 414-420.

Boshoff, W. P., 2007, "Time-dependent behaviour of ECC," Dissertation, Stellenbosch University.

Boshoff, W. P., Mechtcherine, V., and Zijl, G.P.A.G., 2009, "Characterising the time-dependent behaviour on the single fibre level of SHCC: Part 1: Mechanism of fibre pull-out creep," Cement Concrete Research, V.39, pp. 779–786.

Boshoff, W. P., Mechtcherine, V., and Zijl, G.P.A.G., 2009, "Characterising the time-dependent behaviour on the single fibre level of SHCC: Part 2: Rate effects in fibre pull-out tests," Cement Concrete Research, V.39, pp. 787–797.

Cusson, D., 2008. "Effect of blended cements on effectiveness of internal curing of HPC. ACI SP-256, Internal Curing of High-Performance Concretes: Laboratory and Field Experiences," American Concrete Institute, pp. 105–120.

Craeye, B., & De Schutter, G., 2008, "Experimental evaluation of mitigation of autogenous shrinkage by means of a vertical dilatometer for concrete." Eight International Conference 70 on Creep, Shrinkage and Durability Mechanics of Concrete and Concrete Structures, CRC Press/Balkema, pp. 909–914.

Emmons, P. H., and Sordyl, D. J., 2006, “The State of the Concrete Repair Industry, and a Vision for its Future,” Concrete Repair Bulletin, July-Aug. 2006, pp. 7-14.

Euclidchemical.com, 2020. [Online]. Available: https://www.euclidchemical.com/fileshare/ProductFiles/Tds/Plastol_6400.pdf. [Accessed: 09- Oct- 2020].

Gcpat.com, 2020, "ADVA® 140M | GCP Applied Technologies". [Online]. Available: https://gcpat.com/en/solutions/products/adva-high-range-water-reducers/adva-140m. [Accessed: 09- Oct- 2020].

Jun, P., Mechtcherine, V., 2007, “Behaviour of SHCC under repeated tensile loading.” RILEM PRO 53, HPFRCC5. Mainz, Germany, pp 97–104.

Kabele, P., Novák, L., Němeček, J., and Kopeckỳ, L., 2006, “Effects of chemical exposure on bond between synthetic fiber and cementitious matrix,” Proc ICTRC’2006. 1st International RILEM Conference on Textile Reinforced Concrete, Aachen, Germany, RILEM Publications S.A.R.L, pp. 91–100.

Kabele, P., Novák, L., Němeček, J., and Pekař, J. 2007, “Multiscale experimental investigation of deterioration of fiber-cementitious composites in aggressive environment,” Proceedings of MHM 2007: Modeling of heterogeneous materials with applications in construction and biomedical engineering, 25–27 June 2007, Prague, Czech Republic, pp 270–271.

Keoleian, G. A., Kendall, A., Dettling, J. E.; Smith, V. M., Chandler, R. F., Lepech, M. D., and Li, V. C., 2005, “Life Cycle Modeling of Concrete Bridge Design: Comparison of ECC Link Slabs and Conventional Steel Expansion Joints,” Journal of Infrastructure Systems, ASCE, V. 11, No. 1, pp. 51-60.

Kunieda, M., Denarie´, E., Bruhwiler, E., and Nakamura, H., 2007, “Challenges for SHCC: deformability versus matrix density,” RILEM PRO 53, HPFRCC5, Mainz, Germany, pp. 31–38.

Lepech, M., Li, V. C., 2005, “Water permeability of cracked cementitious composites,” In: Proceedings of ICF11, Turin, Italy, pp. 113–130.

Lepech, M. and Li, V. C., 2006, “Durability and Long Term Performance of Engineered Cementitious Composites,” Proceedings of International RILEM workshop on HPFRCC in structural applications, Proceedings of Int'l RILEM workshop on HPFRCC in structural applications, RILEM SARL, pp. 165-174. http://hdl.handle.net/2027.42/84787

Lepech, M. and Li, V. C., 2008, “Large Scale Processing of Engineered Cementitious Composites,” ACI Material Journal, Vol. 105, pp. 358–366.

Li, M. and Li, V.C., 2011, “High-Early-Strength Engineered Cementitious Composites for Fast, Durable Concrete Repair-Material Properties,” ACI Material Journal, V. 108, No. 1, pp. 3-12.

Li, V.C., 1993, “From micromechanics to structural engineering – the design of cementitious composites for civil engineering applications.” JSCE J. Struct. Mech. Earthq. Eng. V. 10 No. I-24, pp. 37s–48s.

Li, V.C., 2019, “Engineered Cementitious Composites (ECC): Bendable Concrete for Sustainable and Resilient Infrastructure” Berlin, Germany: Springer-Verlag GmbH, 2019.

Li, V.C., Wang, S., Wu, C., 2001, “Tensile strain-hardening behaviour of polyvinyl alcohol engineered cementitious composites (PVA-ECC),” ACI Material Journal, V. 98, pp. 483–492.

Li, V.C., 2003, “On engineered cementitious composites (ECC). A review of the material and its applications.” J. Adv. Concr. Technol. V. 1, No. 3, pp. 215–230.

Li, V. C., 2004, “High Performance Fiber Reinforced Cementitious Composites as Durable Material for Concrete Structure Repair,” International Journal for Restoration of Buildings and Monuments, V. 10, No. 2, pp. 163-180.

Li, V.C., Horikoshi, T., Ogawa, A., Torigoe, S., and Saito, T., 2004, “Micromechanics-based durability study of polyvinyl alcohol-engineered cementitious composite.” ACI Material Journal, V.101, pp. 242–248.

Li, V.C. and Li, M., 2011, “Cracking and Healing of Engineered Cementitious Composites under chloride environment,” ACI Materials Journal, V. 108, pp. 333-340.

Lim, C., Kim J., and Seo, T., 2016, “Prediction of concrete adiabatic temperature rise characteristic by semi-adiabatic temperature rise test and FEM analysis” Constr. Build Mater. V. 125, pp. 679-689.

Liu, H., Zhang, Q., Li, V., Su, H., and Gu, C., 2017, “Durability Study on Engineered Cementitious Composites (ECC) under sulfate and chloride attack,” Construction and building materials. V.133, pp. 171-181.

Maalej, M., Ahmed, S. F. U., Paramasivam, P., 2002, “Corrosion durability and structural response of functionally-graded concrete beams,” Journal of Advanced Concrete Technology, V.1, No. 3, pp. 307–316.

Mechtcherine, V., Silva, F., Müller, S., Jun, p., and Filhon, R. D. T., 2012, “Coupled Strain Rate and Temperature Effects on the tensile behavior of Strain-Hardening Cement-Based Composited with PVA fibers,” Cement and Concrete Research, V. 42, pp. 1417-1427.

Mehta, P. K., and Burrows, R. W., 2001, "Building Durable Structures in the 21st Century," Concrete International, V. 23, No. 3, pp. 57-63.

Mihashi, H., Nishiyama, N., Kobayashi, T., and Hanada, M., 2002, "Development of a Smart Material to Mitigate Thermal Stress in Early Age Concrete," Control of Cracking in Early Age Concrete, Balkema, Rotterdam, pp. 385-392.

Miyazato, S., and Hiraishi, Y., 2005, "Transport properties and steel corrosion in ductile fiber reinforced cement composites," In: Proceedings of ICF11, Turin, Italy.

Neithalath, N., 2006, "Analysis of moisture transport in mortars and concrete using sorption-diffusion approach," ACI Material Journal, V. 103 No. 3, pp. 209–217.

Němeček, J., Kabele, P., Kopeckŷ, L., and Bittnar, Z., 2006 "Micromechanical properties of calcium leached engineered cementitious composites," RILEM PRO 49, Honolulu, Hawaii, USA, pp. 205–211.

Němeček, J., Kabele, P., Kopeckŷ, L., and Bittnar, Z., 2007 "Effect of chemical exposure on fiber reinforced cementitious matrix," In: Proceedings of SEMC 2007 The Third International Conference on Structural Engineering, Mechanics and Computation, 10–12 September 2007, Cape Town, South Africa.

Neville, A. M., 1996, "Properties of Concrete." London: Pearson.

Porras, Y., Jones, C., Schmiedeke, N., 2020, "Freezing and Thawing Durability of High Early Strength Portland Cement Concrete," J. Civ. Eng., V. 32, No. 5,

Qadri, F., 2020, "Durable High Early Strength Concrete via Internal Curing Approach using Saturated Lightweight and Recycled Concrete Aggregates," Sage Publications, Inc., V. 2674, No. 7, pp 67-76.

Rapoport, J., Aldea, C., Shah, S. P., Ankenman, B., Karr, A. F., 2001, "Permeability of cracked steel fiber-reinforced concrete," Technical Report Number 115, National Institute of Statistical Sciences.

Sahmaran, M., Li, M., Li, V. C., 2007, "Transport properties of engineered cementitious composites under chloride exposure," ACI Materials Journal, V. 104, No. 6, pp. 604–611.

Sahmaran, M., Li, V. C., and Andrade, C., 2008, "Corrosion resistance performance of steel-reinforced engineered cementitious composite beams," ACI Material Journal, V. 105, No. 3, pp. 243–250.

Sahmaran, M., Li, V. C., 2008, "Durability of mechanically loaded engineered cementitious composites under high alkaline environment," Cement Concrete Composites, V. 30, No. 2, pp. 72–81.

Sahmaran, M., Lachemi, M, and Li, V. C., 2009, "Assessing the Durability of Engineered Cementitious Composites Under Freezing and Thawing Cycles," Journal ASTM International, V. 6, No. 7, doi:10.1520/JAI102406.

Sahmaran, M., Lachemi, M, Hossain, K., and Li, V. C., 2009, "Internal Curing of Engineered Cementitious Composites for Prevention of Early Age Autogenous Shrinkage Cracking," Cement and Concrete Research, V. 39, pp. 893-901.

Sahmaran, M., Lachemi, M, and Li, V. C., 2010, "Assessing Mechanical Properties and Microstructure of Fire-Damaged Engineered Cementitious Composites," ACI Materials Journal, V. 107, No. 3, pp. 297-304.

Sahmaran, M., Özbay, E., Yücel, H.E., Lachemi, M. Li, V. C., 2011, "Frost resistance and microstructure of Engineered Cementitious Composites: Influence of fly ash and micro poly-vinyl-alcohol fiber," Journal of Materials in Civil Engineering, V. 23 No. 12, pp. 1735–1745.

Sahmaran, M., Yücel, H.E., Demirhan, S., Arik, T. M., and Li, V. C., 2012, "Combined Effect of Aggregate and Mineral Admixtures on Tensile Ductility of Engineered Cementitious Composites," ACI Materials Journal, pp. 627–637.

Sahmaran, M., Özbay, E., Yücel, H.E., Lachemi, M. Li, V. C., 2012, "Effect of fly ash and PVA fiber on microstructural damage and residual properties of engineered cementitious composites exposed to high temperatures," Cement and Concrete Composites, V. 34, pp. 156–165.

Sahmaran, M. Al-Emam, M., Yildirim, G., Şimşek, Y. E., Erdem, T. K., and Lachemi, M., 2013, "High-Early-Strength Ductile Cementitious Composites with Characteristics of Low Early-Age Shrinkage for Repair of Infrastructures," Mat and Struct, V. 48, No. 5, pp. 1398-1403.

Shanahan, N., Bien-Aime, A., Buidens, D., Meagher, T., Sedaghat, A., Riding, K., & Zayed, A., 2016, "Combined Effect of Water Reducer-Retarder and Variable Chloride-Based Accelerator Dosage on Rapid Repair Concrete Mixtures for Jointed Plain Concrete Pavement." Materials in Civil Engineering, V. 28 No. 7.

Taffese, W. and Sistonen, E., 2013, "Service Life Prediction of Repaired Structures Using Concrete Recasting Method: State-Of-The-Art" Procedia Engineering, V. 57, pp. 1138-1144.

Tian, Q., & Jensen, O. M., 2008, "Measuring autogenous strain of concrete with corrugated moulds. Microstructure Related Durability of Cementitious Composites," pp. 1501–1511.

Wang, S. and Li, V.C., 2006, "High-Early-Strength Engineered Cementitious Composites," ACI Materials Journal, V. 103, No. 2, pp. 97-105.

Wang, S. and Li, V. C., 2006, "Polyvinyl alcohol fiber reinforced engineered cementitious composites: material design and performances," RILEM PRO 49, Honolulu, Hawaii.

Weimann, M.B., Li, V. C., 2003, "Hygral behavior of engineered cementitious composites (ECC)," International Journal of Restorative Building Monuments, V. 9, No. 5, pp. 513–534.

Weimann, M.B., Li, V. C., 2003, "Drying Shrinkage and Crack Width of Engineered Cementitious Composites (ECC)," Proceeding of International Symposium, "Brittle Matrix Composites 7", ZTUREK RSI and Woodhead Publications, Warsaw, pp. 37-46.

Weiss, W. J., Borischevsky, B. B., & Shah, S. P., 1999, "The influence of a shrinkage reducing admixture on the early-age behavior of high performance concrete," Fifth International Symposium on the Utilization of High Strength/High Performance Concrete, Sandefjord, Norway, pp. 1418–1428.

Yon, H., Kim, S., Lee, Y., and Rokugo, K., 2011, "Tensile Behavior of Synthetic Fiber-Reinforced Strain-Hardening Cement-Based Composite after Freezing and Thawing Exposure," Cold Regions Science and Technology, V. 67, pp. 49-57.

Yu, K., Dai, J., Lu, Z., and Leung, C. K. Y., 2014, "Mechanical Properties of Engineered Cementitious Composites Subjected to Elevated Temperatures," Journal of Materials in Civil Engineering, V. 27, No. 10.

Yu, K., Dai, J., Lu, Z., and Poon, C., 2018, "Rate-dependent tensile properties of ultra-high performance engineered cementitious composites (UHP-ECC)," Cement Concrete Composites, V. 93, pp. 218-234.

Zhang, J., Gong, C., Guo, Z., and Zhang, M., 2009, "Engineered Cementitious Composite with Characteristic of Low Drying Shrinkage," Cement and Concrete Research, V. 39, pp. 303-312.

Zijl, G.P.A.G.V., Wittmann, F.H., Oh, B.H., Kabele, P., Filho, R.D.T., Fairbairn, E.M.R., Slowik, V., Ogawa, A., Hoshiro, H., Mechtcherine, V., et al., 2012, "Durability of strain-hardening cement-based composites (SHCC)," Material Structures, V. 45, pp. 1447–1463.